Molecular Crystals and Liquid Crystals

Publication details, including instructions for authors and subscription information:
http://www.tandfonline.com/loi/gmcl20

Multifrequency Epr and Endor on Transient Radicals and Radical Pairs in Liquid Crystals and Proteins: Structure and Dynamics of Cofactors in Natural and Artifical Photosynthesis

Klaus Möbius [a]

[a] Department of Physics, Free University Berlin, Arnimallee 14, Berlin, D-14195, Germany

Version of record first published: 18 Oct 2010

To cite this article: Klaus Möbius (2003): Multifrequency Epr and Endor on Transient Radicals and Radical Pairs in Liquid Crystals and Proteins: Structure and Dynamics of Cofactors in Natural and Artifical Photosynthesis, Molecular Crystals and Liquid Crystals, 394:1, 1-17

To link to this article: http://dx.doi.org/10.1080/15421400390193639

Mol. Cryst. Liq. Cryst., Vol. 394, pp. 1–17, 2003

ISSN 1542-1406 print/1563-5287 online
DOI: 10.1080/15421400390193639

Taylor & Francis
Taylor & Francis Group

MULTIFREQUENCY EPR AND ENDOR ON TRANSIENT RADICALS AND RADICAL PAIRS IN LIQUID CRYSTALS AND PROTEINS: STRUCTURE AND DYNAMICS OF COFACTORS IN NATURAL AND ARTIFICAL PHOTOSYNTHESIS

Klaus Möbius
Free University Berlin, Department of Physics, Arnimallee 14, D-14195 Berlin, Germany

Hotly debated issues in the area of biological electron transfer (ET) involve questions of how long-range ET processes proceed along pathways that incorporate non-covalently linked cofactors interacting with their protein microenvironment. To contribute answers to such questions, time-resolved EPR (TREPR) experiments at various microwave frequency/magnetic field settings have been performed. In this overview, representative examples of this work from our laboratory are given which comprise transient intermediates of light-induced ET in (i) bacterial photosynthetic reaction centers and (ii) biomimetic model complexes. In these complexes the donor and acceptor components are tethered together either covalently via cyclohexenyl bridges or non-covalently via Watson-Crick base-pairing. The studies are aiming at broadening our knowledge of structure-dynamics-function relationships associated with ET processes. It is demonstrated that high-field TREPR opens new perspectives in elucidating complex photochemical ET reactions with different paramagnetic states and species involved.

Keywords: time-resolved EPR; electron transfer; photosynthesis; model system

Over the last years, numerous coworkers – students, postdocs, colleagues – from different parts of the world have contributed to the work presented. To all of them I want to express my gratitude. Their individual share in the work is highly appreciated and becomes evident by the references cited. I remember with affection and gratitude the lively discussions with Pier Luigi Nordio on molecular motion in protein systems during my extended stay in Padova in 1997. Over the years his knowledge and enthusiasm strongly affected our work, and his friendship and encouragement will remain in our memory. Financial support of our work by the Deutsche Forschungsgemeinschaft (SPP 1051, Sfb 498) and Volkswagenstiftung (I/73 146) is gratefully acknowledged.

1. INTRODUCTION

For a proper understanding of the electronic and three-dimensional structures and the dynamics of paramagnetic molecules, the determination of the tensor components of the Zeeman, fine, hyperfine and quadrupole interactions are of fundamental importance. In isotropic liquid solution only the trace of the interaction tensors can be measured directly from EPR (electron paramagnetic resonance) and ENDOR (electron nuclear double resonance) line positions. Consequently, traceless interaction tensors, such as quadrupole and fine structure interactions, escape direct detection unless an anisotropic environment is provided. Single crystals would be an optimum choice but are often not available for interesting (bio)molecular systems.

As an intriguing aspect, liquid crystals with nematic mesophase can be used as an alternative to single crystals to, at least partially, align the solute molecules. For this situation, the line positions become also dependent on the magnitude of the anisotropic interactions and on the degree of alignment at a particular temperature. For example, the first determination of ^{14}N quadrupole couplings in organic radicals was achieved by ENDOR in liquid crystals [1]. Of particular importance are ^{2}H quadrupole couplings as sensitive probes for hydrogen-bond networks of cofactors in their microenvironment. Consequently, much work has been done to establish correlations between the deuterium quadrupole coupling, $e^2q_DQ_D$, and the H $\cdots$ O lengths in an H-bond of deuterated molecules, see for example [2]. Although for typical H-bond situations in organic systems, $e^2q_DQ_D$ couplings amount to only 100 kHz, they can, nevertheless, be measured with high precision by ENDOR in liquid crystals [3] or polycrystalline samples [4]. In fact, for small quadrupole couplings ENDOR is the only method of choice, since it is basically an NMR experiment. EPR, on the other hand, is not suitable in this respect because, to first order, the quadrupole interaction shifts all levels equally that are connected by EPR transitions. The potential of multifrequency ENDOR for elucidating H-bond networks of cofactors in their protein binding sites is currently being exploited by several groups working on photosynthetic reaction centers, for example by applying ^{1}H-ENDOR [5,6] or ^{2}H-ENDOR [7] to frozen-solution samples.

Another intriguing aspect of using liquid-crystal solvents in EPR spectroscopy is related to their nematic potential which hinders molecular reorientation by orders of magnitude [8]. For light-induced electron transfer (ET) reactions in model donor-acceptor complexes of photosynthesis, this inherent property of nematic liquid crystals can be used to retard the dielectric relaxation, and thereby the relevant ET rates, into the solvent-controlled adiabatic limit [9]. In this case ET and spin dynamics can

be observed within the ns-μs EPR time window. Thus, to a certain extent, liquid crystals can be used to mimic the "solvent" anisotropy of *in vivo* protein complexes with their ET cofactors embedded in the anisotropic binding sites of neighbouring amino acids.

In the following we will focus on time-resolved multifrequency EPR on photo-induced donor/acceptor transients in photosynthetic reaction centers and biomimetic model systems to elucidate relations between structure, dynamics and function of important electron-transfer processes. The examples of this overview are selected with the intention to give a state-of-the-art report of our recent EPR activities, in particular at high magnetic fields. They comprise (i) anisotropic librational motion of quinone ions in photosynthetic reaction centers, (ii) electron-transfer and spin-dynamics characteristics in natural and biomimetic photosynthetic radical pairs.

The examples refer to collaborative work of our group with the groups of W. Lubitz (TU Berlin), H. Kurreck and D. Stehlik (FU Berlin), T.F. Prisner (Frankfurt/M.), and H. Levanon (Jerusalem).

2. EXPERIMENTAL

Continuous-wave (CW) and time-resolved (TR) multifrequency EPR experiments were performed at 9.5 GHz (X-band), 95 GHz (W-band), and 360 GHz, the corresponding Zeeman fields for $g = 2$ systems are 0.34 T, 3.4 T, and 12.8 T, respectively. In analogy to modern high-field/high-frequency NMR, high-field/high-frequency EPR becomes necessary when g-factor differences or g-tensor anisotropies, Δg, of the radicals involved are smaller than the inhomogeneous hyperfine-broadened line widths, $\Delta B_{1/2}^{hf}$. In order to resolve the inhomogeneously broadened spectra and observe the contributions from individual radical sites and/or g-tensor orientations, the Zeeman field, B_0, has to be chosen high enough to allow the condition

$$\frac{\Delta g}{g_{iso}} \cdot B_0 > \Delta B_{1/2}^{hf}$$

to be fulfilled [10–12].

The bioorganic systems studied have $g \approx 2$, and relative g anisotropies, $\Delta g/g$, are as small as 5×10^{-4} for quinone anion radicals and even smaller for chlorophyll and porphyrin cation radicals. Hence, for slowly tumbling or disordered biomolecules with typical EPR line width around 1 mT, 95-GHz or even 360-GHz high-field EPR is mandatory to resolve canonical orientations in the spectra. Our laboratory-built TREPR spectrometers with pulsed laser excitation and variable temperature capabilities have been

described earlier, *i.e.*, for X-band in ref. [13], for W-band in ref. [14]. Both spectrometers reach 10 ns time resolution. For 360-GHz EPR, the quasi-optical spectrometer was only used in CW-mode of operation [15].

The preparation and characterization of the bacterial reaction centers (RCs) of the photosynthetic purple bacterium *Rhodobacter* (Rb.) *sphaeroides* R-26, in which the non-heme Fe^{2+} has been replaced by Zn^{2+} (Zn-RC) have been described elsewhere [16].

The synthesis of the covalently linked Zn-porphyrin-quinone dyad and triad donor-acceptor complexes and of the non-covalently linked Watson-Crick base-paired donor-acceptor complexes, consisting of properly functionalized Zn-porphyrin and dinitrobenzene, are described in refs. [17] and [18], respectively. These complexes are constructed with the aim to mimic essential features of primary photosynthetic electron transfer (ET), see below. The sample solutions were carefully deoxygenated either by high-vacuum destillation or flushing with argon. As nematic liquid-crystal solvent, E-7 (Merck) was used. The alignment of the nematic mesophase occurred in the Zeeman fields of the EPR experiments. The light excitation of the donor molecules for generating charge-separated radical-pairs states in natural and artificial photosystems was provided by a frequency-doubled Nd:YAG laser (Quanta Ray) with 5 ns light pulses (532 nm, 1–5 mJ, 10 Hz repetition) that illuminate the sample in the EPR resonator via a quartz light fiber. The protocol for light generation of the individual quinone acceptors, $Q_A^{-\bullet}$ and $Q_B^{-\bullet}$, in Zn-RCs of *Rb. sphaeroides* is more elaborate, but has been described in detail recently [19,20].

3. RESULTS AND DISCUSSION

1. Anisotropic Dynamics of Quinone Acceptors in their Binding Sites of Photosynthetic Reaction Centers

Three billion years before green plants evolved photosynthetic energy conversion could already be achieved by certain photosynthetic bacteria, for instance the purple bacterium *Rb. sphaeroides*. These early photosynthetic organisms are one-cellular protein-bound donor-acceptor complexes that contain only one RC for light-induced charge separation. They cannot split water like green-plant photosystems, but rather use hydrogen sulfide or organic compounds as electron donors to reduce CO_2 to carbohydrates with the help of sunlight and bacteriochlorophyll (BChl) as biocatalyst.

In intact bacterial RCs, after light excitation an electron is transferred from the primary donor, the BChl *a* "special pair" dimer, P_{865}, to the primary quinone acceptor, Q_A, on a 200-ps time scale. On a much slower time

scale ($\approx$100 μs) the electron is handed over to a secondary quinone acceptor, Q_B, which successively accepts a second electron from Q_A and two protons from the cytoplasm to ultimately leave the Q_B binding site. The site is reoccupied by a new quinone from the quinone pool in the membrane (for a review of the photophysics of bacterial photosynthesis, see [21]).

Hence, quinones play an important role in primary photosynthesis. In RCs of ***Rb. sphaeroides***, $Q_A$and Q_B are the same ubiquinones-10; their different redox functions in the ET processes are obviously induced by different interactions with their protein environment, mainly by forming specific hydrogen-bond networks at their binding sites. The functional role of this H-bond network as pathway for the specific ET routes can be elucidated by site-specific mutations by which RCs are created with modified cofactor-protein interactions. Worldwide intense research is being done to characterize wild-type and mutant RCs in terms of their three-dimensional and electronic structure in relation to their ET function, for example by X-ray crystallography [22,23], FTIR [24–27], as well as EPR and ENDOR spectroscopies [10,21,28–30]. These research activities improved considerably our understanding of the structure-dynamics-function relationships in primary photosynthesis. This also holds for the binding sites of the primary and secondary quinones, Q_A and Q_B, in ***Rb sphaeroides*** to which we will restrict ourselves in the following discussion.

High-field EPR and ENDOR experiments on the quinone radical anions in frozen RC solutions were performed at W-band frequencies to measure anisotropic g and hyperfine tensor components, respectively [31]. The aim was to learn about the anisotropic interactions with the protein environment, such as hydrogen bonding to specific amino acid residues, and about the motional dynamics of the quinones in their binding sites. Owing to the high Zeeman magnetoselection capability of W-band EPR, a high degree of orientational selectivity is achieved that is unaccessible by X-band EPR. The measured g tensor components follow the sequence $g_{xx} > g_{yy} > g_{zz}$, where x is along the -C = O bond direction, and z is perpendicular to the quinone plane.

Exploiting the Zeeman magnetoselection even further, W-band pulsed Davies-type ENDOR was performed at the rather well separated canonical peaks of the powder EPR spectrum. At least for the g_{xx} and g_{zz} canonical field positions, the ENDOR spectra are single-crystal like, *i.e.*, the orientational selections of molecules show narrow distributions. When varying the solvent (protic and aprotic, with and without perdeuteration), characteristic changes of hyperfine couplings (predominantly along the y-direction) and g tensor components (predominantly along the x-direction) could be discerned. They are attributed to hydrogen-bond formation at the lone-pair orbitals on the oxygens.

Besides *static* cofactor-protein interactions as a controlling factor for enzyme activity, *dynamic* properties of cofactors in their binding sites are also of particular relevance. This also holds for the primary processes in photosynthesis if the time constant of a characteristic molecular motion becomes comparable to one of the time constants in the ET chain for charge separation or recombination. For this reason, there is an increasing interest in the slow-motional modes of thermal fluctuations of protein-cofactor complexes. They may affect the electron tunnelling mechanism and thereby the biological function. EPR studies of such cofactor dynamics can build upon the profound knowledge of slow-motion effects in complex solvents accumulated earlier by the groups of J.H. Freed [32–34] and P.L. Nordio [35–37].

In order to learn more about slow motions of the quinone cofactors in photosynthesis, the anisotropic stochastic oscillatory motions of $Q_A^{-\bullet}$ in frozen RC solutions of *Rb. sphaeroides* have been studied by pulsed 95-GHz high-field EPR methods [31]. The two-dimensional field-swept electron spin echo (ESE) technique was chosen for this experiment because it directly reveals the homogeneous line width parameter T_2 and, due to the high field, resolves its variation over the powder spectrum. The strength of the ESE technique to elucidate anisotropic molecular motion in solids or proteins has been recognized earlier [34,38–40]. ESE is favorably performed at high magnetic fields because of enhanced spectral resolution of small g-tensor anisotropies and high time resolution of pulsed high-field EPR [31]. For high-field EPR on the quinone cofactor ion radicals, the dominant T_2 relaxation contribution stems from fluctuations of the Zeeman interaction. The magnitudes of the T_2 contributions are determined by random walk on the surface of the $Q^{-\bullet}$ g-tensor ellipsoid. This leads to time- and angular-dependent fluctuations, δg, that translate to fluctuations of the Larmor frequency, $\delta\omega$, of the electron spins. Obviously, the Larmor frequency fluctuations will be minimal for $Q_A^{-\bullet}$ oscillations around the principal axes *x*,*y*,*z*. Hence, the T_2 values will be the largest along the directions of the respective axes of oscillation. Thus, the maximum of T_2 in the g_{xx} region (see Fig. 1) reveals that, at 115 K, the wobbling motion of $Q_A^{-\bullet}$ predominantly occurs around the *x*-direction, *i.e.*, along the -C=O bond direction. From the high-resolution X-ray structure of the Q_A binding site [41] one can conclude that this finding reflects the hydrogen bond situation of the Q_A site: the most probable H-bond partners of Q_A are histidine (M219) and alanine (M260). They provide the *x*-axis of torsional fluctuations of Q_A at low temperature, and influences of the isoprenoid tail seem to be negligible because of its high flexibility. This result is consistent with the H-bond characteristics of the Q_A binding site determined by other spectroscopic methods, such as NMR [42] and FTIR [43,44] on ^{13}C labeled systems.

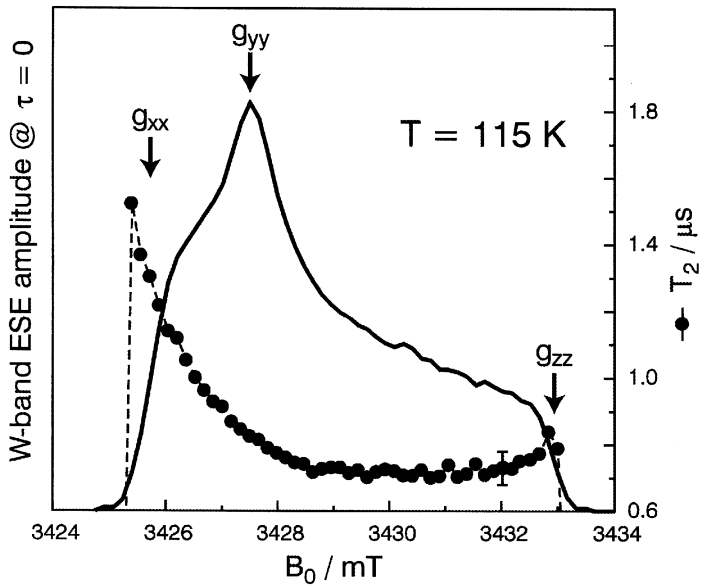

FIGURE 1 Field-swept two-pulse electron-spin-echo (ESE) spectrum of $Q_A^{-\bullet}$ in frozen-solution Zn-RCs from *Rb. sphaeroides* [20] (T = 115 K). The extrapolated $\tau = 0$ slice of the ESE-detected EPR amplitudes and the T_2 relaxation times are depicted as function of the Zeeman field B_0. For details, see [20].

Most recently, we have extended this high-field ESE work to the Q_B site in Zn-RCs of *Rb. sphaeroides* with the aim to look for conformational changes of the Q_B site in the ET photocycle [19]. By comparing the T_2 anisotropies of $Q_A^{-\bullet}$ and $Q_B^{-\bullet}$, detailed information about the H-bond networks of the two binding sites could be obtained. The anisotropy of the T_2 relaxation due to anisotropic stochastic fluctuations of the quinones in their H-bond networks is temperature dependent.

As is seen from Figure 2, for $Q_A^{-\bullet}$ and $Q_B^{-\bullet}$ the mono-exponential echo decays at 120 K have different orientation-dependent time constants. Their temperature-dependent characteristics are consistent with charge-induced reorientations of the quinone and amino acids of the Q_B site, as had been observed recently by comparing dark-adapted and light-adapted RCs of *Rb. sphaeroides* by X-ray crystallography [22]. Such reorientations do not occur at the Q_A site [22]. The light-induced reorientations of $Q_B^{-\bullet}$ are mechanistically of great importance for the photosynthetic ET process and explain the "Kleinfeld effect" on the ET recombination rates for $Q_B^{-\bullet}$: In 1984 Kleinfeld had observed that the recombination rate of $Q_B^{-\bullet}$ to the neutral ground state was increased by several orders of magnitude when

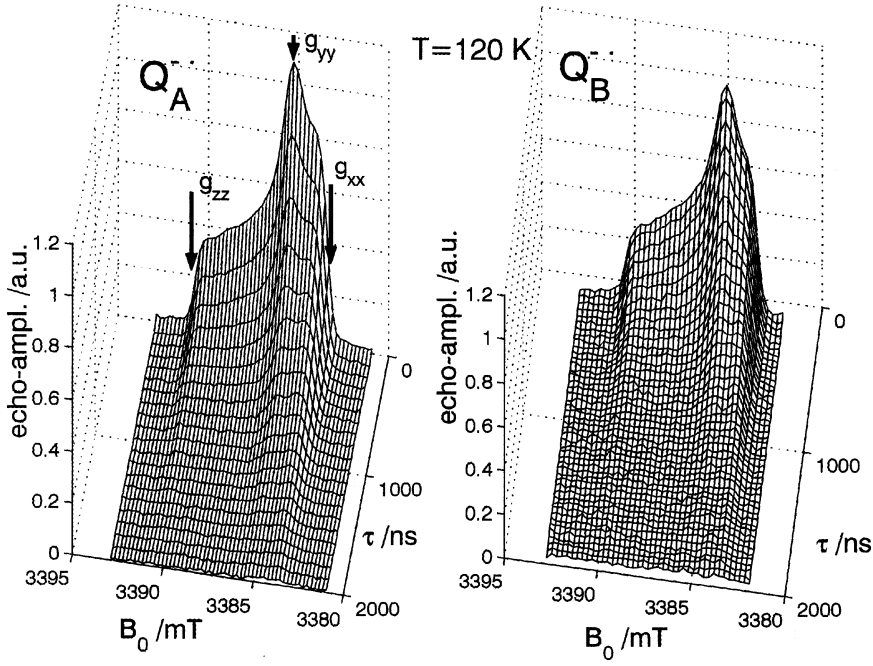

FIGURE 2 Two-dimensional W-band ESE-detected EPR spectra of $Q_A^{-\bullet}$ and $Q_B^{-\bullet}$ in Zn-RCs from *Rb. sphaeroides* at 120 K [19]. The echo-decays of $Q_A^{-\bullet}$ and $Q_B^{-\bullet}$ as function of B_0 differ by their g_{xx} values and time constants. For details, see [19]. (The figure was kindly provided by A. Schnegg, FUB).

RCs were frozen under illumination, *i.e.*, in the charge-separated state, as compared to RCs frozen in the dark, *i.e.*, in the ground state [22].

With increasing temperature the T_2 relaxation of both $Q_A^{-\bullet}$ and $Q_B^{-\bullet}$ becomes less anisotropic. To rationalize this observation, a motional model is proposed [19,31] in which the orientation-dependent relaxation originates in reorientational fluctuations around the quinone's specific H-bonds to surrounding amino acids of the binding site. At 120 K the dominant H-bond determines the axis about which small-angle fluctuation take place. To a good approximation, this is the *x*-axis of the quinone g-tensor. The fluctuations are approximated by a two-site jump with rms angle $\pm\delta X$. The higher the temperatures the weaker the H-bonds. As a consequence, at higher temperatures the libration axis itself is less precisely fixed in space and may deviate from its equilibrium position. Therefore, we assume that the quinone *x*-axis is distributed on a cone whose aperture increases with increasing temperatures. Fore more details, see [19].

2. Correlated Radical-Pair State of the Primary Donor and Acceptor in Rb. sphaeroides Reaction Centers

In spite of their large separation of approx. 28 Å in the photosynthetic membrane, the primary donor "special pair", $P_{865}^{+\bullet}$, and primary acceptor, $Q_A^{-\bullet}$, experience spin correlation in their radical-pair state owing to their weak mutal dipolar and exchange interactions. This can be exploited by TREPR to obtain valuable structure information of transient intermediates in the light-initiated photocycle of primary ET [45,46].

Pulsed W-band EPR experiments on the short-lived $P_{865}^{+\bullet}Q_A^{-\bullet}$ radical pair in frozen Zn-RC solution of *Rb. sphaeroides* allowed the determination of the three-dimensional structure of the charge-separated donor-acceptor system [16]. The high-field EPR spectra were recorded by the field-swept two-pulse echo technique. The charge-separated radical pairs $P_{865}^{+\bullet}Q_A^{-\bullet}$ were generated by 10-ns laser flashes. Their TREPR spectrum is strongly electron spin-polarized because the transient radical pair is suddenly born in a spin-correlated non-eigenstate of the spin Hamiltonian with pure singlet character. Such spin-polarized spectra with lines in enhanced absorption and emission (see Fig. 3) contain important structural information of magnitude and orientation of the g-tensors of the two radical partners, $P_{865}^{+\bullet}$ and $Q_A^{-\bullet}$, with respect to each other and to the dipolar axis z_d connecting the two radicals (see Fig. 3). Several parameters critically determine the lineshape of the polarization pattern [16], such as the principal values of the g and dipolar coupling tensors, the exchange coupling J, and the inhomogeneous line width of both radicals. These parameters were determined independently in order to obtain meaningful simulations of the spin-polarized spectra. From earlier time-resolved EPR measurements [11] on the radical pair $P_{865}^{+\bullet}Q_A^{-\bullet}$, at X-band (9.5 GHz), K-band (24 GHz) and Q-band (35 GHz), g-tensor orientations could not be extracted unambiguously from simulations of the spin-polarized spectra. This was mainly because of strongly overlapping lines, even when deuterated samples were used to reduce hyperfine contributions. In the pulsed W-band experiments, however, the Zeeman field is strong enough to largely separate the inhomogeneously broadened contributions from $P_{865}^{+\bullet}$ and $Q_A^{-\bullet}$. Thus, the overall spectrum is dominated by the anisotropies and differences of the two g-tensors. Thereby the interpretation of the polarized spectrum is simplified and allows an unambiguous analysis of the tensor orientations. The most important result of this high-field EPR study is that, within an error margin of ± 0.3 Å, no light-induced structural changes of the $Q_A^{-\bullet}$ site with respect to $P_{865}^{+\bullet}$ occur, as compared to the ground-state configuration $P_{865}Q_A$. This finding is in accordance with recent results from various other studies including pulsed EPR [10] and X-ray crystallography [22], and is in contrast to the situation of the Q_B site (see above).

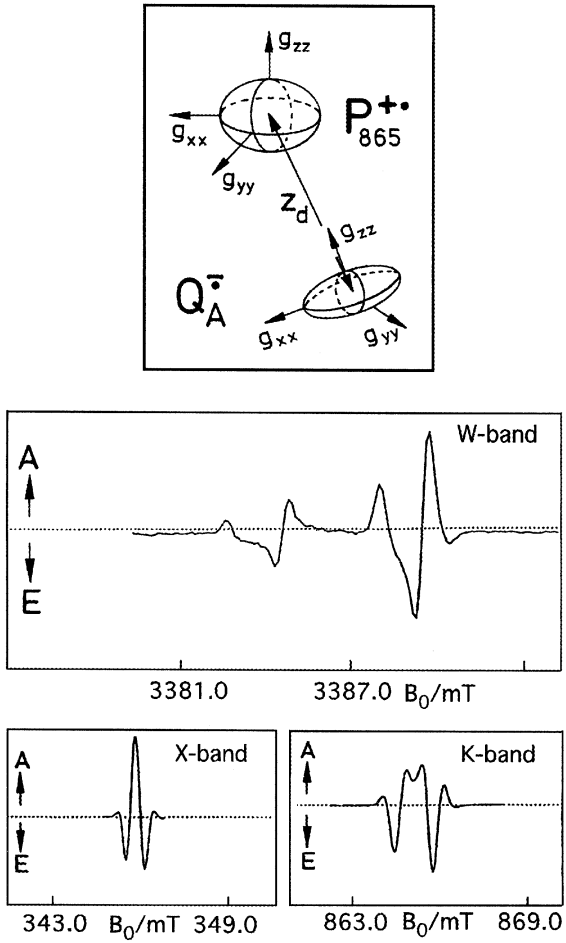

FIGURE 3 Schematic respresentation of the relative orientation of the g-tensors and dipolar axis z_d of the light-generated transient radical pair $P^{+\bullet}_{865}Q^{-\bullet}_{A}$ in *Rb. sphaeroides*. Its spin-polarized EPR spectrum of deuterated Zn-RCs in frozen solution (T = 140 K), recorded about 200 ns after the laser pulse, is shown for X-, K- and W-band field/frequency settings [11,16] (A, E stand for absorption, emission, respectively). For details, see [16].

Generally, pulsed high-field EPR experiments on spin-correlated coupled radical pairs allow to detect ET-induced structural changes in the relative orientation of donor and acceptor with high precision, even for disordered samples. Such information is very desirable for a detailed understanding of the ET characteristics on the molecular level. One should

keep in mind that the charge-separated radical-pair state represents the working state for ET recombination processes. This general statement applies, of course, also to donor-acceptor model systems.

3. Biomimetic Donor-Acceptor Model Systems

The complexity of the natural photosynthetic RCs has prompted a worldwide study of model systems in an attempt to reproduce essential features of the biological target and to understand the structure-dynamic-function relationship of natural and artificial photosynthesis. Much of our current understanding of this relationship stems from studies of donor-acceptor model systems in homogeneous media (isotropic and liquid crystalline) that might mimic some of the primary events in natural photosynthesis with their high quantum yield and long-living charge-separated states. It is clear by now that such model studies provide complementary information to *in vivo* studies – and *vice versa*.

In the following, we will concentrate on biomimetic donor-acceptor complexes that are (i) covalently linked by spacer groups and (ii) that are not covalently linked but rather by H-bond networks of Watson-Crick-type base pairing, thus better mimicking the natural RC situation. The protein bath of the RC and its effect on the ET characteristics was modeled by the anisotropic environment of the nematic phase of the liquid-crystal solvent (E-7).

Owing to the high spectral and time resolution of our laboratory-built multifrequency TREPR spectrometers (10–50 ns), electron-spin-polarization (ESP) effects associated with the transient photoreaction products could be observed, as well as their development with time (ns to μs) after the laser pulse. The lineshape of the emission/enhanced absorption spectra and its change with time contains a wealth of structural information via g-tensors, hyperfine couplings, dipolar and exchange interactions of radical-pair intermediates. The multifrequency TREPR approach enabled us to separate the various contributions (g-factor and hyperfine) to dominant ESP mechanisms. Under controlled environmental conditions (solvent polarity, temperature, medium anisotropy) the role of the microenvironment in long-range ET could be elucidated.

(i) Covalently linked donor-acceptor complexes

These donor-acceptor complexes, studied in cooperation with the Kurreck group, comprise porphyrin-spacer-quinone dyads, triads and, most recently, tetrads with long-living charge-separated radical-pair (RP) states. Figure 4 shows examples of cyclohexylene-bridged porphyrine-quinone dyad and triad model systems that were investigated by 9.5- and 95-GHz TREPR [47]. The spin-polarized spectra of the light-induced transient spin-correlated RP states could be detected in polar solvents below the melting

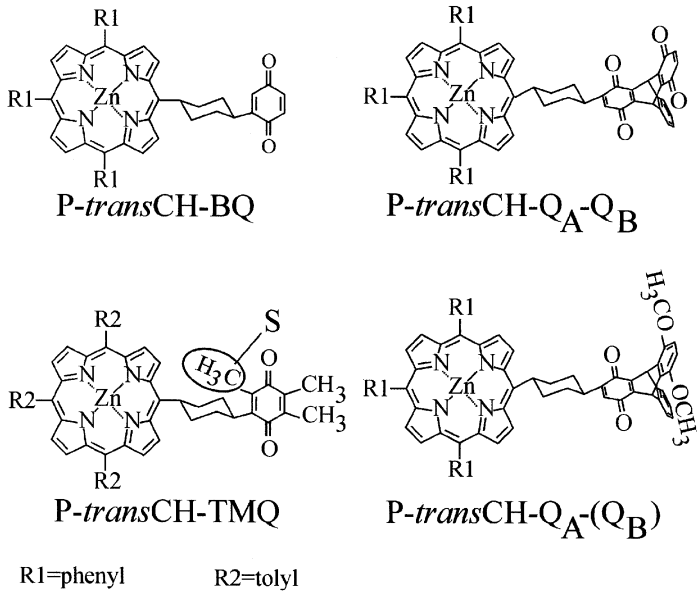

FIGURE 4 Molecular structure of covalently linked Zn-porphyrin-quinone dyad and triad model systems. The methyl substituent, S, restricts motion about the cyclohexylene link and the quinone. For details, see [17].

point and in the soft-glass nematic phase of the liquid crystal E-7. They reveal that the model systems form strongly exchange-coupled RPs, whose TREPR lineshapes are determined mainly by fast electron recombination together with both spin-lattice relaxation and modulation of the exchange interaction. Most probably, this is due to contributions from spin-rotation interaction and, moreover, is dependent on the molecular orientation with respect to the magnetic field. This relaxation anisotropy is related to anisotropic motion of the quinone in the solvent cage. The results allow conclusions to be drawn concerning the precursor state of the light-induced ET (triplet-state porphyrin after fast intersystem-crossing from the photoexcited singlet state) and the molecular dynamics and flexibility of the systems. To yield long-lived RP states that would mimic photosynthetic ET, the modulation of exchange and spin-rotation interactions have to be suppressed by reducing the molecular flexibility of the complex, for example by bulky substituents (labeled S in Fig. 4).

The lifetime of the charge-separated radical-pair state (approx. 5 μs) is rather long for a system in which the electrons are separated by only 10–15 Å. When comparing this with the much longer lifetime of the radical-pair state $P_{865}^{+\bullet}Q_A^{-\bullet}$ (approx. 100 μs) in RCs of *Rb. sphaeroides*, one has to keep

in mind that the mechanisms which lead to these lifetimes are very different for the model and *in vivo* systems: Also in natural photosynthesis the primary charge-separated radical pair, $P^{+\bullet}H^{-\bullet}$, is electronically strongly coupled, but it is born in the singlet state (H is a bacteriopheophytin). A long lifetime of an electron-separated state is achieved by the second ET step to the Q_A acceptor, by which the distance between the two unpaired electrons is strongly increased. This $P^{+\bullet}Q_A^{-\bullet}$ radical pair, therefore, is electronically weakly coupled. By contrast, the charge-separated states of the porphyrin-quinone dyad and triad model systems are formed by ET from triplet porphyrin and trapped as triplet state of a strongly coupled radical pair, from which charge recombination to the ground state is spin-forbidden. It is interesting to note that, in contrast to the covalently bridged systems, certain Watson-Crick base-paired donor-acceptor systems are electronically weakly coupled, but nevertheless show rather fast electron separation rates and, with only one ET step, provide a long-lived radical-pair state (see below).

We believe that the covalently linked triad systems represent a good starting point for creating long-lived radical-pair states in tetrad systems of covalently linked porphyrins and quinones. In such 4-component model systems an additional ET step is possible, resulting in an even larger separation of the two electrons. The longer the lifetimes of the dyad and triad radical pairs, the higher the probability for the additional ET step. Since the lifetime in the dyad and triad systems is limited by the motion-induced triplet-singlet transitions described above, the important strategy for long lifetimes is to restrict molecular flexibility. On the other hand, a certain degree of molecular flexibility is necessary for the first ET step to take place at all. The challenge for constructing suitable tetrad systems is to allow for enough flexibility to initiate ET, but simultaneously to provide enough rigidity to restrict the lifetime-limiting triplet-singlet transitions. The investigation of a novel porphyrin-quinone tetrad system, which has been synthesized by the Kurreck group [48], by TREPR at several microwave frequencies is currently under way in the Berlin laboratory.

(ii) Watson-Crick type base-paired donor-acceptor aggregates

An alternative approach to modeling photosynthetic ET processes, which may be considered as being more biomimetic than covalently linked complexes, involves selforganized supramolecular porphyrin-acceptor aggregates in which molecular recognition proceeds via base-pairing, stabilized by multiple hydrogen-bonding interactions. Figure 5 (left) shows, as an example, a base-paired porphyrin-dinitrobenzene supramolecular donor-acceptor complex which has been studied by multifrequency TREPR after selective pulsed laser excitation [18]. The complex is expected to

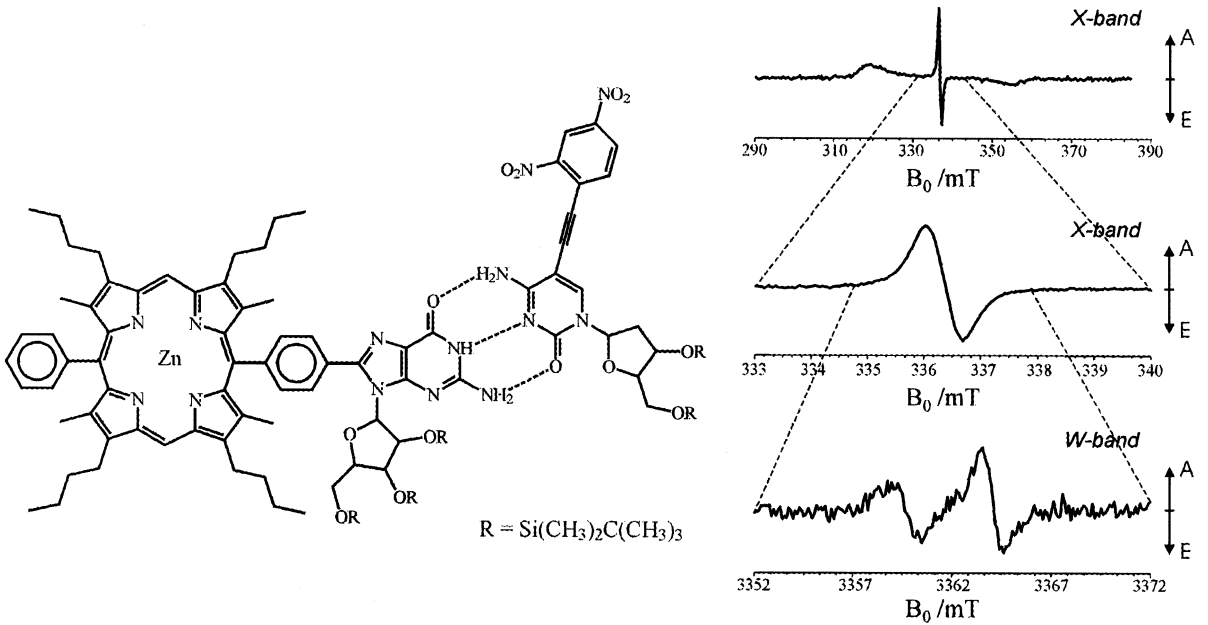

FIGURE 5 Left: Guanine-functionalized Zn-porphyrin H-bonded to cytosine-functionalized dinitrobenzene via Watson-Crick type base-pairing. Right: TREPR spectra of this H-bonded complex in the nematic phase of the liquid crystal E-7 after light-excitation (T = 280 K). *Top*: SCRP spectrum superimposed on the triplet spectrum (X-band). *Middle*: Expanded SCRP spectrum (X-band). *Bottom*: Resolved SCRP spectrum at W-band. For details, see [18].

consist of selforganized Zn-porphyrin and nitrobenzene components because they are functionalized by appropriate guanine and cytosine residues to allow for Watson-Crick base pairing. The threefold H-bonding network should provide substantial rigidity of the aggregate. The functionalized donor and acceptor components were synthesized by the Sessler group [49].

The spin-polarized TREPR spectra at X-band and W-band are shown in Figure 5 (right), taken 250 ns after the laser pulse at 280 K in E-7. In the nematic phase of the this solvent, 532 nm photoexcitation of the Zn-porphyrin moiety yields a broad absorptive/emissive spectrum and a superimposed narrow derivative-like signal. The rise of the narrow signal is accompanied by the decay of the broad signal, which is ascribed to the lowest excited triplet state of the Zn-porphyrin. These findings are rationalized in terms of intra-ensemble ET occurring from the Zn-porphyrin triplet-state donor to the dinitrobenzene acceptor, and by specific spin-polarization effects. The narrow EPR signal is attributed to a long-distance charge separated, but still spin-correlated radical pair (SCRP) with a lifetime of several 100 μs at room temperature. The theoretical analysis of the process predicts that the observed SCRP signal is the superposition of the signals of the RP participants, which remains unresolved at X-band EPR. In order to identify unambiguously the partners of the RP complex and thereby clarify the origin of the SCRP signal, high-field TREPR experiments at W-band were performed. At these high Zeeman fields the g-factors of both RP partners could be completely resolved (2.0025, 2.0052), see Figure 5 (right). By comparison with known g-factor data, the results prove that indeed a self-assembled complex of Zn-porphyrin and dinitrobenzene is formed through multiple H-bonding by nucleobase pairing. The high time resolution of our W-band EPR spectrometer (≈10 ns) allowed to identify the porphyrin triplet state as the precursor state of the photoinduced long-distance ET.

To summarize: These experiments on biomimetic systems and photosynthetic reaction centers show that high-field time-resolved EPR opens new directions in the elucidation of complex photochemical reactions with different magnetic states and species involved.

4. CONCLUSIONS

In this overview we have indicated how state-of-the-art multifrequency EPR and ENDOR, both in CW and TR mode of operation, in particular at high magnetic fields and microwave frequencies, provide detailed information on electronic and geometric structures and dynamics of transient radicals and radical pairs that occur in light-induced electron-

transfer processes in photosynthetic reaction centers and biomimetic donor-acceptor complexes. Thereby our understanding of the relation between structure, dynamics and function is considerably improved. This is especially true with respect to the fine-tuning of electronic properties of donors and acceptors by means of weak interactions with their protein environment, such as hydrogen bonding to specific amino acid residues.

The anisotropic environment of cofactors in their protein scaffold can, in part, be modeled by anisotropic solvents such as nematic liquid crystals. This allows to measure even traceless interactions, such as quadrupole couplings of ^{14}N and ^{2}H nuclei, by ENDOR in solution, thereby getting access to another sensitive probe for the electronic structure of complex systems, in addition to the hyperfine and g-tensor probes. Moreover, nematic liquid crystals offer an advantage in investigations of photo-initiated electron-transfer processes by time-resolved EPR: Spin-polarized spectra of radicals, triplets and radical pairs can be observed over wide temperature ranges up to room temperature, thereby revealing important information about electron-transfer and spin dynamics in elementary (bio)chemical reactions. A particular strength of multifrequency time-resolved EPR in determining structure-dynamics-function relationships of biosystems should be stressed: Not only ground-state properties can be elucidated, but also properties of transient intermediates. They can be observed in real-time while the transients are staying in their *working states* on biologically relevant time scales.

REFERENCES

[1] Dinse, K. P., Möbius, K., Plato, M., Biehl, R., & Haustein, H. (1972). *Chem. Phys. Lett.*, *14*, 196.
[2] Soda, G. & Chiba, T. (1969). *J. Phys. Soc. Japan*, *26*, 249.
[3] Biehl, R., Lubitz, W., Möbius, K., & Plato, M. (1977). *J. Chem. Phys.*, *66*, 2074.
[4] Mayas, L., Plato, M., Winscom, C. J., & Möbius, K. (1978). *Mol. Phys.*, *36*, 753.
[5] Rohrer, M., MacMillan, F., Prisner, T. F., Gardiner, A. T., Möbius, K., & Lubitz, W. (1998). *J. Phys. Chem.*, *102*, 4648.
[6] Müh, F., Lendzian, F., Roy, M., Williams, J. C., Allen, J. P., & Lubitz, W. (2002). *J. Phys. Chem. B.*, *106*, 3226.
[7] Isaacson, R. & Feher, G. (2002). (UC San Diego), personal communication.
[8] Martin, A. J., Meier, G., & Saupe, A. (1971). *Symp. Faraday Soc.*, *5*, 119.
[9] Marcus, R. A. & Sutin, N. (1985). *Biochim. Biophys. Acta*, *811*, 265.
[10] Levanon, H. & Möbius, K. (1997). *Annu. Rev. Biophys. Biomol. Struct.*, *26*, 495.
[11] Stehlik, D. & Möbius, K. (1947). *Annu. Rev. Phys.Chem.*, *48*, 745.
[12] Prisner, T., Rohrer, M., & MacMillan, F. (2001). *Annu. Rev. Phys. Chem.*, *52*, 279.
[13] Elger, G., Törring, J., & Möbius, K. (1998). *Rev. Sci. Instrum.*, *69*, 3637.
[14] Prisner, T. F., Rohrer, M., & Möbius, K. (1994). *Appl. Magn. Reson.*, *7*, 167.
[15] Fuchs, M. R., Prisner, T. F., & Möbius, K. (1999). *Rev. Sci. Instrum.*, *70*, 3681.

[16] Prisner, T. F., van der Est, A., Bittl, R., Lubitz, W., Stehlik, D., & Möbius, K. (1995). *Chem. Phys.*, *194*, 361.
[17] Fuhs, M., Elger, G., Osintsev, A., Popov, A., Kurreck, H., & Möbius, K. (2000). *Mol. Phys.*, *98*, 1025.
[18] Berg, A., Shuali, Z., Asano-Someda, M., Levanon, H., Fuhs, M., Möbius, K., Wang, R., Brown, C., & Sessler, J. L. (1999). *J. Am.Chem. Soc.*, *121*, 7433.
[19] Schnegg, A., Fuhs, M., Rohrer, M., Lubitz, W., Prisner, T. F., & Möbius, K. (2002). *J. Phys. Chem. B*, in print.
[20] Rohrer, M., Gast, P., Möbius, K., & Prisner, T.F. (1996). *Chem. Phys. Lett.*, *259*, 523.
[21] Hoff, A.J. & Deisenhofer, J. (1997). *Phys. Reports*, *287*, 1.
[22] Stowell, M. H. B., McPhillips, T. M., Rees, D. C., Soltis, S. M., Abresch, E. C., & Feher, G. (1997). *Science*, *276*, 812.
[23] Lancaster, C. R. D. & Michel, H. (2001). In: *Handbook of Metalloproteins*, Messerschmidt, A., Huber, R., Poulos, T., & Wieghardt, K. (Eds.), John Wiley: Chichester, 119–135.
[24] Thibodeau, D. L., Nabedryk, E., Hienerwadel, T., Lenz, F., Mäntele, W., & Breton, J. (1990). *Biochim. Biophys. Acta*, *1020*, 243.
[25] Breton, J. & Nabedryk, E. (1996). *Biochim. Biophys. Acta*, *1275*, 84.
[26] Gerwert, K. (2000). In: *Infrared and Raman Spectroscopy of Biological Materials*, Gremlich, H.-U. & Yan, B. (Eds.), Marcel Dekker: New York, 193–230.
[27] Mezzetti, A., Nabedryk, E., Breton, J., Okamura, M. Y., Paddock, M. L., Giacometti, G., & Leibl, W. (2002). *Biochim. Biophys. Acta*, *1553*, 320.
[28] Lubitz, W. & Feher, G. (1999). *Appl. Magn. Reson.*, *17*, 1.
[29] Möbius, K. (2000). *Chem. Soc. Rev.*, *29*, 129.
[30] Weber, S. (2000). *Spec. Period. Repts., Electron Paramagn. Reson.*, *17*, 43.
[31] Rohrer, M., Gast, P., Möbius, K., & Prisner, T. F., (1996). *Chem. Phys. Lett.*, *259*, 523.
[32] Polimeno, A. & Freed, J. H. (1995). *J. Phys. Chem.*, *99*, 10995.
[33] Polimeno, A., Moro, G. J., & Freed, J. H. (1995). *J Chem. Phys.*, *102*, 8094; *104*, 1090 (1996)
[34] Freed, J. H. (2000). *Annu. Rev. Phys. Chem.*, *51*, 655.
[35] Nordio, P. L. & Polimeno, A. (1996). *Int. J. Quant. Chem.*, *60*, 321.
[36] Nordio, P. L. & Polimeno, A. (1996). *Mol. Phys.*, *88*, 315.
[37] Nordio, P. L., Polimeno, A., & Saielli, G. (1997). *J. Photochem. Photobiol. A*, *105*, 269.
[38] Millhauser, G. L. & Freed, J. H. (1984). *J. Chem. Phys.*, *81*, 37.
[39] Dzuba, S. A., Tsvetkov, Yu. D., & Maryasov, A. G. (1992). *Chem. Phys. Lett.*, *188*, 217.
[40] Dzuba, S. A. (1996). *Phys. Lett. A*, *213*, 77.
[41] Ermler, U., Fritzsch, G., Buchanan, S. K., & Michel, H. (1994). *Structure*, *2*, 925.
[42] van Liemt, W. B. S., Boender, G. J., Gast, P., Hoff, A. J., Lugtenburg, J., & de Groot, H. J. M. (1995). *Biochemistry*, *34*, 10229.
[43] Breton, J., Boullais, C., Burie, J.-R., Nabedryk, E., & Mioskowski, C. (1994). *Biochemistry*, *33*, 14378.
[44] Brudler, R., de Groot, H. J. M., van Liemt, W. B. S., Steggerda, W. F., Esmeijer, R., Gast, P., Hoff, A. J., Lugtenburg, J., & Gerwert, K. (1994). *EMBO J.*, *13*, 5523.
[45] Hore, P. J. (1989). In: *Advanced EPR—Applications in Biology and Biochemistry*, Hoff, A. J. (Ed.), Elsevier: Amsterdam, 405–440.
[46] Salikhov, K. M., Bock, L. H., & Stehlik, D. (1990). *Appl. Magn. Reson.*, *1*, 195.
[47] Fuhs, M., Elger, G., Osintsev, A., Popov, A., Kurreck, H., & Möbius, K. (2002). *Mol. Phys.*, *98*, 1025.
[48] Wiehe, A., Senge, M. O., Schäfer, A., Speck, M., Tannert, S., Kurreck, H., & Röder, B. (2001). *Tetrahedron*, *57*, 10089.
[49] Asano-Someda, M., Levanon, H., Sessler, J. L., & Wang, R. (1998). *Mol. Phys.*, *95*, 935.